Appl. Phys. A (2015) 120:669–674
DOI 10.1007/s00339-015-9236-7

Applied Physics A
Materials Science & Processing

Fabrication of three-dimensional micro-Rogowski coil based on femtosecond laser micromachining

Xiangwei Meng[1] · Qing Yang[1] · Feng Chen[1] · Chao Shan[1] · Keyin Liu[1] · Xun Hou[1]

Received: 5 February 2015 / Accepted: 13 May 2015 / Published online: 22 May 2015

Abstract This paper reports an arbitrary-shape designable fabrication of three-dimensional (3D) micro-Rogowski coil inside silica glass by means of femtosecond laser wet etches and metal microsolidics. The dimension of the fabricated micro-Rogowski coil is 800 μm, and the aspect ratio of the structure reaches about 300. The alloys of Bi/In/Sn/Pb with high melting point were used as the conductive metal. The inductance of micro-Rogowski coil is 113.58 nH at 10 kHz and 14.11 nH at 120 MHz, respectively. The embedded 3D micro-Rogowski coils can be easily integrated with other microelectrical, mechanical and optical systems, which could be widely applied in MEMS, sensors and lab-on-chips.

1 Introduction

In recent years, metal microwiring has attracted much attention due to its significance in microcircuitry and electronic interconnection [1–3]. The microwire could meet the growing requirements of highly integrated microcircuit, which would improve the integration level of the microdevices and reduces the size of the microsystems effectively. The microcoil sensors are usually used as inductors to enhance radio-frequency (RF) response signals and created magnetic fields to improve imaging capability in magnetic resonance imaging (MRI) systems and various types of advanced electromagnetic microsensors and microactuators [4–6].

Rogowski coil is a special kind of helical coil sensor, which can measure the current with high values and even the transient current of pulses as short as several nanoseconds [6–8]. Micro-Rogowski coil is a key device with typically complex three-dimensional (3D) metal microstructures in developing miniaturized current measurement system [9, 10]. It consists of a helical coil and the wire with the lead from one end returning through the center of the coil to the other end, so that both terminals are at the same end of the coil.

Several techniques have been used to fabricate microwires, which have already greatly contributed to integrated circuits. Generally, lithography and electroplating methods were adopted to realize planar metal wires on planar substrates [11–13]. However, the planar microcoils result in inhomogeneous magnetic field and low inductance values. In comparison with planar microcoils, the 3D solenoid microcoils can generate a stronger and more uniform magnetic field; it also provides a higher inductance and lower resistance [12, 14]. The process consists of UV depth lithography, and electroplating method could be also improved to fabricate 3D microcoils [15]. However, these methods always require expensive equipments and have complicated procedures. Although the straight solenoid microcoils can be made by winding metal microwire around pillars [16, 17], the method is difficult to fabricate complex solenoid microcoils, such as micro-Rogowski coils [18].

In this paper, we present the solution to fabricate complex 3D microcoils by FLWE and metal microsolidics technology. An alloy with high melting point is injected into the microchannel to achieve the conductor wire, which can reduce the impact of the Joule heat and get a higher

✉ Feng Chen
chenfeng@mail.xjtu.edu.cn

[1] State Key Laboratory for Manufacturing System Engineering and Key Laboratory of Photonics Technology for Information of Shaanxi Province, School of Electronics and Information Engineering, Xi'an Jiaotong University, No 28 Xianning West Road, Xi'an 710049, People's Republic of China

working temperature of the devices. By writing the laser focus along a predesigned pattern in silica glass and wet etching process, the micro-Rogowski coil with coil core is achieved. The inductance and resistance of micro-Rogowski coil is measured by an impedance analyzer, and the measurement results show the good electromagnetic property of micro-Rogowski coil. Moreover, the unique ability of this method can be widely used for fabricating a variety of complex 3D microcoils to miniaturize the size of devices in various engineering applications.

2 Method and experiment

Silica glass ($10 \times 10 \times 1$ mm^3) was used in the experiment. The sample was fixed on a computer-controlled 3D stage. A Ti:sapphire pulsed laser with 50 fs, 800 nm and 1 kHz is vertically focused into the sample by a 100× objective lens (NA = 0.9, Nikon). The sample is fixed onto a computer-controlled 3D stage. In the laser-writing process, the 3D pattern was directly written by translating the sample along the predesigned path, as shown in Fig. 1a. Subsequently, the sample was immersed into hydrofluoric acid (HF) solution and the modified materials were dissolved. The microchannel consequently formed in a few hours (Fig. 1b).

For preparing microsolidics, a series of alloys with different melting points (47, 70, 94 and 125 °C) were chosen as the metallic conductors. These alloys contain different percentages of Bi/In/Sn/Pb. In order to seal the extra access ports and create the connector for the following injection process, a polydimethylsiloxane (PDMS) film was firstly prepared on the sample surface having microchannel (Fig. 1c). Then, the microchannel devices and the alloy were put in the electrically heated drying oven; the temperature of the oven was 30 °C higher than the melting point of the alloy. Subsequently, the liquid metal was injected into the microchannel to achieve the conductive microcoils. During this injection process, two syringes were used to inject the liquid metal into the fabricated microchannel. The liquid metal in a syringe was squeezed into the microchannel by a high pressure, and a suction pump in the other entrance sucked the metal simultaneously (Fig. 1d). After the injection process, the alloy was solidified completely at low temperature and the PDMS film was peeled. Then, the inductance and resistance of micro-Rogowski coil is measured by an impedance analyzer. The measure results demonstrate the good electromagnetic property of micro-Rogowski coil.

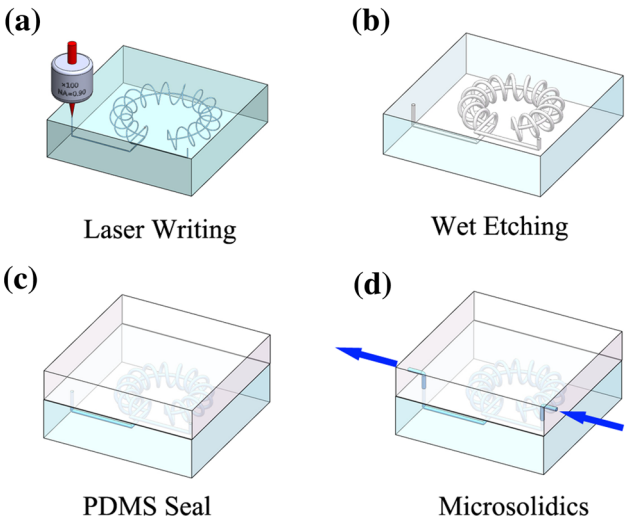

Fig. 1 Schematic diagrams of the fabrication procedures: **a** laser-writing process; **b** complex microchannel is formed by wet etching. **c** PDMS film seals the extra access ports. **d** Alloy microwires fabricated inside silica glass

3 Results and discussions

The fabrication of the microchannel by FLWE process in silica glass consists of two steps: (1) laser writing and (2) wet chemical etching. The propagation of the laser-induced mechanical pressure wave (i.e., shock wave) in silica glass may cause densification and limit destruction around the focus volume of the silica. $O_3 \equiv$ Si-(O)–Si $\equiv O_3$ bridging angles of the SiO_4 tetrahedrons in the modification structure decrease, which increases the reactivity of oxygen because of the deformed configuration of the oxygen's valance electrons. The configuration deformation is considered in terms of the Lewis base, which is more chemically active in reactions with HF acid. Thus, the femtosecond laser-irradiated regions will have a higher etching rate than the un-irradiated regions [19].

To overcome the limitation of the length and uniformity of the microchannel fabricated by the conventional femtosecond laser wet etch process, the control of the microchannel shapes by suitable wobbling of the glass substrate during the irradiation process has been reported in ref [20], which would be time-consuming and increase the diameter of the microchannel. Our group has proposed the improved FLWE process by introducing extra access ports to fabricate the 3D helical microchannel with arbitrary length and uniform diameter [21]. At the top points of the laser scan lines, which are the closest to the upper surface of the sample, the extra access ports were vertically fabricated with lengths of 80 μm, as shown in Fig. 2a. These ports would increase the connections between the laser-induced embedded microstructures and the etchant. When the sample with the embedding laser scanning lines was immersed in the etching solution, HF acid solution could directly flow into the central parts of the channel rapidly

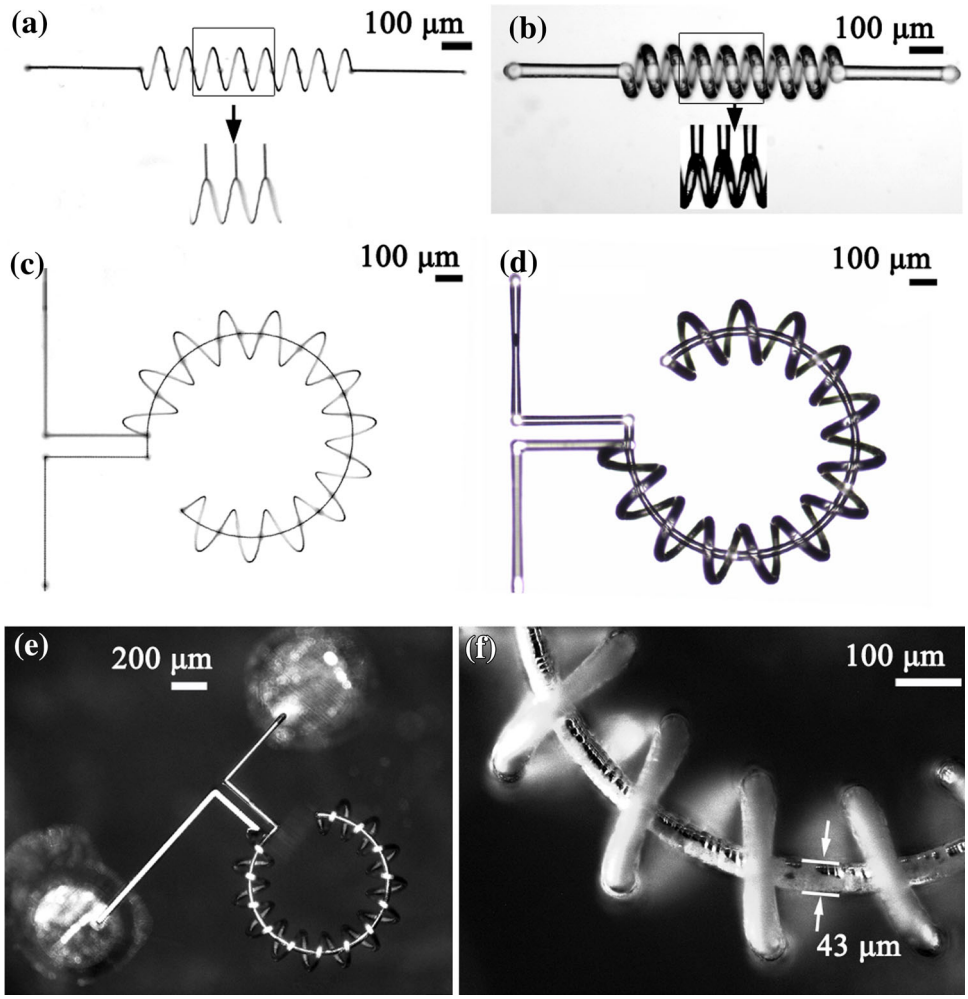

Fig. 2 **a** Optical microscope image of the helical line written by the femtosecond laser. **b** Optical microscope image of the helical microchannel after the wet etching. **c** The top view optical microscope image of Rogowski pattern line. **d** Optical microscope image of the Rogowski pattern microchannel. **e** The optical microscope image of fabricated true 3D micro-Rogowski coil. **f** The local enlarged image of the Rogowski coil

through the extra access ports, which part is voids caused by microexplosion around the focal point of the irradiated laser. So the each part of the microchannel can be etched almost simultaneously [22, 23]. By properly arranging the distance between the extra access ports, microchannels in the silica glass with uniform diameters can be fabricated, which will also overcome the length limitation of the femtosecond laser wet etching process (Fig. 2b). After the etching process, the extra access ports can be polished away or blocked by insulating light-curing adhesive.

In the laser irradiation experiment, the pattern of Rogowski coil with a core was irradiated by the femtosecond laser, as shown in Fig. 2c. The radius of the toroid and the radius of the turn are 400 and 100 μm, respectively. The O-shape helical lines were written, and then, the line returned through the center of the helical lines to the other end. Because of the tightly focused laser and the nature of the nonlinear absorption in the silica glass, the region of the laser-induced breakdown is confined in the focal spot without damage surrounding materials, which enables the O-shape core to pass through the helical coil without contact [24]. The Fig. 2d shows the fabricated microchannel with the structure of the Rogowski coil after the etching process. The diameter of the microchannel is about 43 ± 2 μm, and the etching time is about 230 min. The length of microchannel is about 12.84 mm, so the aspect ratio of the microcoils is up to 300. The area of 3D micro-Rogowski coil is about 0.79 mm^2.

The microsolidics process has been employed to fabricate metallic microstructures in 3D by injecting molten solder into the networks of microfluidic channels in PDMS for the conductive treatment [25, 26]. In the previous work, gallium was chosen as the metallic conductors, because of its low melting point (29.8 °C), low fluid mobility and low resistivity. However, due to the low melting point, the microwire can be easily melted by the Joule heat and ultimately disconnected, which would greatly limit the operating current and working temperature in practical application. In this work, an alloy comprising of different percentages of Bi/In/Sn/Pb with high melting point has been utilized. The extra access ports were sealed by a PDMS film. The injection pressure was produced by a

syringe pump to inject the liquid alloy into the microchannel. Simultaneously, a suction pump was applied to supply a high negative pressure. In the whole microsolidics process, the work temperature should be maintained at a value higher than the melting point of the alloy. After the alloy solidification, the Rogowski coil was fabricated inside the silica glass, as shown in Fig. 2e. Hence, the alloy microwire would have higher operating current and working temperature. The microwire of Rogowski coil with coil core has a good uniformity and continuity even at the circles (Fig. 2f). In this process, the extra access ports were sealed by PDMS, and when the liquid alloy was injected into the microchannel, the air would be trapped and squeezed into extra access ports. The higher air pressure in the ports could prevent the liquid alloy from flowing into the extra access ports. Therefore, the extra access ports would not affect the injection of the liquid metal. The air in the extra access ports leads to the discontinuous dielectric around Rogowski coil, which will influence the electromagnetic field space distribution. To eliminate the negative effect of these extra access ports, the Rogowski line can be written much closer to the surface of the sample and the length of the extra access ports should be as short as possible.

Figure 3a shows the morphology of a line written by the laser on the surface of the sample. In the etching process, the nanostructures and modified materials can be etched out rapidly, owing to their higher selective etch rate. The diameter of the microchannel increases, and the surface roughness decreases, when the modified materials are completely removed. After the etching process, the SEM image shows the good uniformity and smoothness of the microchannel (Fig. 3b). The diameter of the laser-writing line could be adjusted simply by controlling the laser power, and the dependence is shown in Fig. 3c. The line diameter of the laser writing increases linearly with the power. In addition, the diameter of the microchannel with the same laser parameters and different etching times are measured. Figure 3d shows that the diameter of the microchannel increases linearly with the etching time and the diameter of the microchannel could be well controlled by adjusting the etching time.

The inductance can be calculated by the empirical formula:

$$L = \mu_0 N^2 \left(R - \sqrt{R^2 - a^2}\right) \quad (1)$$

where μ_0 is the magnetic constant, R is the major radius of the toroid and a is the minor radius. Hence, the inductance of the micro-Rogowski coil is estimated to be 2.49 nH. The direct current (DC) resistance is measured to be 2.4 Ω by digital multimeter. Figure 4a shows the measurement data of the Rogowski coils by an impedance analyzer. The inductance decreases with the frequency and has a value of 113.58 nH at 10 kHz. The inductance is stable up from 10 to 120 MHz, and the values are 15.38 and 14.11 nH, respectively. The value of the inductance has the same order of magnitude as the estimated value. The resistance increases almost linearly with the frequency due to skin and

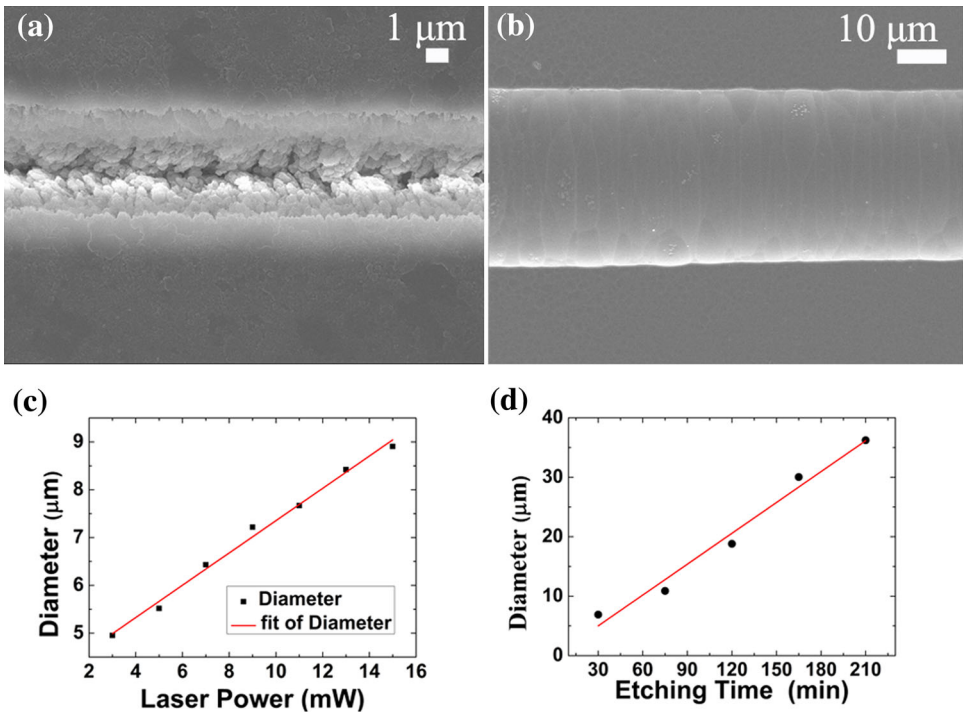

Fig. 3 **a** SEM image of the laser-writing line. **b** SEM images of the channel after the wet etching. **c** The dependence of the diameter of line on the laser power. **d** The evolution of the diameter of the microchannel versus the wet etching time

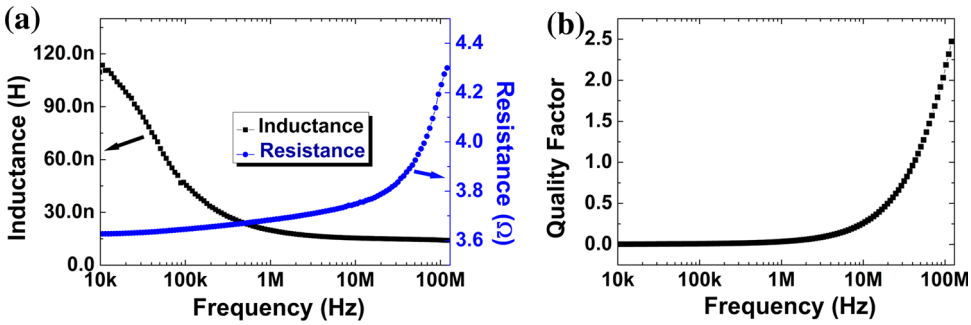

Fig. 4 Measurement data of Rogowski coil. **a** The inductance and the resistance of Rogowski coil; **b** the quality factor

proximity effects. The values are 3.75 Ω at 10 MHz and 4.30 Ω at 120 MHz, respectively, which also has the same order of magnitude as the DC resistance. Quality factor, Q, is the key parameter that determines the efficiency of the inductor device, and it is proportional to the ratio of energy stored to the energy lost per unit time, which can be calculated by the formula:

$$Q = \omega \frac{L}{R} \tag{2}$$

where ω is the frequency. The calculated quality factors of Rogowski coil is plotted in Fig. 4b. The maximal quality factor is measured at frequency of 120 MHz and has a value of 2.47. The voltage produced by the Rogowski coil can be expressed as:

$$V = \frac{-AN\mu_0}{l}\frac{\mathrm{d}I}{\mathrm{d}t} \tag{3}$$

where $A = \pi r^2$ is the area of the turn, N is the number of turns and $l = 2\pi R$ is the length of the winding (the circumference of the ring). $\mathrm{d}I/\mathrm{d}t$ is the rate of change of the current threading the loop. At high frequencies, the inductance of Rogowski coil will decrease its output.

4 Conclusions

In conclusion, true 3D micro-Rogowski coil with a coil core has been fabricated in silica glass by the improved femtosecond laser wet etch (FLWE) and metal microsolidics method. The high aspect ratio and uniformity microchannel were realized by the introduced extra access ports. By controlling the wet etching time and laser power, the turn of the coil and diameter of the complex microchannel could be easily adjusted. An alloy with high melting point was applied to achieve the conductor of the microcoils, so the fabricated microwire can overcome the limitation of operating current and working temperature. Moreover, the inductance of micro-Rogowski coil was measured, and the values are 113.58 nH at 10 kHz and 14.11 nH at 120 MHz, respectively. The quality factor was calculated and has a value of 2.47 at 120 MHz. This work provides a potential route to realize true 3D microcoils inside material and would be beneficial for developing miniaturization and highly integrated microactuators and microsensors.

Acknowledgments This work is supported by the National Science Foundation of China under the Grant Nos. 51335008, 61275008 and 61176113, the Special-funded program on National Key Scientific Instruments and Equipment Development of China under the Grant No. 2012YQ12004706.

References

1. M. Barbic, J.J. Mock, A.P. Gray, S. Schultz, Appl. Phys. Lett. **79**, 1399–1401 (2001)
2. H. Ryan, S.H. Song, A. Zaß, J. Korvink, M. Utz, Anal. Chem. **84**, 3696–3702 (2012)
3. D.H. Kim, Y.S. Kim, J. Wu, Z.J. Liu, J.Z. Song, H.S. Kim, Y.G.Y. Huang, K.C. Hwang, J.A. Rogers, Adv. Mater. **21**, 3703–3708 (2009)
4. V. Badilita, B. Fassbender, K. Kratt, A. Wong, C. Bonhomme, D. Sakellariou, J.G. Korvink, U. Wallrabe, Plos One **7**, e42848 (2012)
5. T.F. Kong, W.K. Peng, T.D. Luong, N.T. Nguyen, J. Han, Lab Chip **12**, 287–294 (2012)
6. A. Salehizadeh, A. Sadighzadeh, M.S. Movahhed, A.A. Zaeem, A. Heidarnia, R. Sabri, M.B. Mahmoudi, H. Rahimi, S. Rahimi, E. Johari, M. Torabi, V. Damideh, J. Fusion Energy **32**, 293–297 (2013)
7. E. Hemmati, S.M. Shahrtash, IEEE Trans. Instrum. Meas. **62**, 71–82 (2013)
8. K. Draxler, R. Styblikova, J. Hlavacek, R. Prochazka, IEEE Trans. Instrum. Meas. **60**, 2434–2438 (2011)
9. S. Tumanski, Meas. Sci. Technol. **18**, R31–R46 (2007)
10. B. Moffat, M. Desmulliez, K. Brown, C. Desai, D. Flynn, A. Sutherland, in *Electronics system-integration technology conference, 2008, IEEE*, vol. 299, pp. 299–304 (2008)
11. C. Leia, Y. Zhoua, X.-Y. Gaoa, W. Dinga, Y. Caoa, Z.-M. Zhoua, H. Choib, Microelectron. J. **37**, 1347–1351 (2006)
12. K. Ehrmann, N. Saillen, F. Vincent, M. Stettler, M. Jordan, F.M. Wurm, P.A. Besse, R. Popovic, Lab Chip **7**, 373–380 (2007)
13. V. Demas, A. Bernhardt, V. Malba, K.L. Adams, L. Evans, C. Harvey, R.S. Maxwell, J.L. Herberg, J. Magn. Reson. **200**, 56–63 (2009)
14. V. Badilita, K. Kratt, N. Baxan, M. Mohmmadzadeh, T. Burger, H. Weber, D. Elverfeldt, J. Hennig, J.G. Korvink, U. Wallrabe, Lab Chip **10**, 1387–1390 (2010)

15. V. Seidemann, S. Buettgenbach, Microelectron. MEMS Technol. (Int. Soc. Opt. Photonics) **4407**, 304–309 (2001)
16. K. Kratt, V. Badilita, T. Burger, J.G. Korvink, U. Wallrabe, J. Micromech. Microeng. **20**, 015021 (2010)
17. S. Waselikowski, K. Kratt, V. Badilita, U. Wallrabe, J.G. Korvink, M. Walther, Appl. Phys. Lett. **97**, 261105 (2010)
18. B.B. Xu, H. Xia, L.G. Niu, Y.L. Zhang, K. Sun, Q.D. Chen, Y. Xu, Z.Q. Lv, Z.H. Li, H. Misawa, H.B. Sun, Small **6**, 1762–1766 (2010)
19. A. Marcinkevicius, S. Juodkazis, M. Watanabe, M. Miwa, S. Matsuo, H. Misawa, J. Nishii, Opt. Lett. **26**, 277–279 (2001)
20. K.C. Vishnubhatla, N. Bellini, R. Ramponi, G. Cerullo, R. Osellame, Opt. Express **17**, 8685–8695 (2009)
21. S. He, F. Chen, K. Liu, Q. Yang, H. Liu, H. Bian, X. Meng, C. Shan, J. Si, Y. Zhao, Opt. Lett. **37**, 3825–3827 (2012)
22. F. Chen, C. Shan, K. Liu, Q. Yang, X. Meng, S. He, J. Si, F. Yun, X. Hou, Opt. Lett. **38**, 2911–2914 (2013)
23. S. He, F. Chen, Q. Yang, K. Liu, C. Shan, H. Bian, H. Liu, X. Meng, J. Si, Y. Zhao, J. Micromech. Microeng. **22**, 105017 (2012)
24. R.R. Gattass, E. Mazur, Nat. Photonics **2**, 219–225 (2008)
25. A.C. Siegel, D.A. Bruzewicz, D.B. Weibel, G.M. Whitesides, Adv. Mater. **19**, 727–733 (2007)
26. K. Liu, Y. Zhao, Q. Yang, F. Chen, S. He, X. Fan, L. Li, C. Shan, H. Bian, in *NEMS 2013 8th IEEE International Conference*, pp. 677–680